

Domain wall mobility in nanowires: transverse versus vortex walls

R. Wieser, U. Nowak and K. D. Usadel

Theoretische Tieftemperaturphysik, Gerhard-Mercator-Universität Duisburg, 47048 Duisburg, Germany

(Dated: November 1, 2018)

The motion of domain walls in ferromagnetic, cylindrical nanowires is investigated numerically by solving the Landau-Lifshitz-Gilbert equation for a classical spin model in which energy contributions from exchange, crystalline anisotropy, dipole-dipole interaction, and a driving magnetic field are considered. Depending on the diameter, either transverse domain walls or vortex walls are found. The transverse domain wall is observed for diameters smaller than the exchange length of the given material. Here, the system behaves effectively one-dimensional and the domain wall mobility agrees with a result derived for a one-dimensional wall by Slonczewski. For low damping the domain wall mobility decreases with decreasing damping constant. With increasing diameter, a crossover to a vortex wall sets in which enhances the domain wall mobility drastically. For a vortex wall the domain wall mobility is described by the Walker-formula, with a domain wall width depending on the diameter of the wire. The main difference is the dependence on damping: for a vortex wall the domain wall mobility can be drastically increased for small values of the damping constant up to a factor of $1/\alpha^2$.

PACS numbers: 75.10.Hk, 75.40.Mg, 75.60.Ch

Arrays of magnetic nanowires are possible candidates for patterned magnetic storage media [1, 2]. For these nanowires and also for other future magneto-electronic devices the understanding of domain wall motion and mobility is important for the controlled switching of the nanostructure. In a recent experiment the velocity of a domain wall in a NiFe/Cu/NiFe trilayer was investigated using the GMR effect [3]. The measured velocities were compared with the Landau-Lifshitz formula for domain wall motion [4]. This comparison was used to determine the damping constant of the trilayer, a quantity which is usually not known a priori. However, several formulas for the velocity of a domain wall can be found in the literature [4, 5, 6, 7, 8] which are derived in different limits and all in (quasi) one-dimensional models neglecting the possible influence of non-uniform spin structures within the domain wall. Thus the question arises in how far these formulas are applicable to real three dimensional domain structures. To shed some light onto this problem we numerically investigate the domain wall mobility in nanowires starting from a three dimensional local spin model.

In the following we consider a classical spin model with energy contributions from exchange, crystalline anisotropy, dipole-dipole interaction, and a driving magnetic field. Such a spin model for the description of magnetic nanostructures [9] can be justified following different lines: on the one hand it is the classical limit of a quantum mechanical, localized spin model, on the other hand it might be interpreted as the discretized version of a micromagnetic continuum model, where the charge distribution for a single cell of the discretized lattice is approximated by a point dipole. For certain magnetic systems their description in terms of a lattice of magnetic moments may even be based on the mesoscopic structure of the material, especially when a particulate medium is described.

However, our intention is not to describe a particular material but to investigate a general model Hamiltonian which is

$$\mathcal{H} = - J \sum_{\langle ij \rangle} \mathbf{S}_i \cdot \mathbf{S}_j - \mu_s \mathbf{B} \cdot \sum_i \mathbf{S}_i - D_e \sum_i (S_i^z)^2 - \omega \sum_{i < j} \frac{3(\mathbf{S}_i \cdot \mathbf{e}_{ij})(\mathbf{e}_{ij} \cdot \mathbf{S}_j) - \mathbf{S}_i \cdot \mathbf{S}_j}{r_{ij}^3}, \quad (1)$$

where the $\mathbf{S}_i = \boldsymbol{\mu}_i/\mu_s$ are three dimensional magnetic moments of unit length on a cubic lattice.

The first sum is the ferromagnetic exchange between nearest neighbors with coupling constant J . The second sum is the coupling of the spins to an external magnetic field B , the third sum represents a uniaxial anisotropy, here, with $D_e > 0$, favoring the z axis as easy axis of the system, and the last sum is the dipolar interaction where $w = \mu_0 \mu_s^2 / (4\pi a^3)$ describes the strength of the dipole-dipole interaction. The \mathbf{e}_{ij} are unit vectors pointing from lattice site i to j and r_{ij} is the distance between these lattice sites in units of the lattice constant a .

The underlying equation of motion for magnetic moments which we consider in the following is the Landau-Lifshitz-Gilbert (LLG) equation,

$$\frac{\partial \mathbf{S}_i}{\partial t} = - \frac{\gamma}{(1 + \alpha^2)\mu_s} \mathbf{S}_i \times \left[\mathbf{H}_i(t) + \alpha(\mathbf{S}_i \times \mathbf{H}_i(t)) \right], \quad (2)$$

with the gyromagnetic ratio $\gamma = 1.76 \times 10^{11} (\text{Ts})^{-1}$, the dimensionless damping constant α (after Gilbert), and the internal field $\mathbf{H}_i(t) = -\partial \mathcal{H} / \partial \mathbf{S}_i$.

We simulate cylindrical systems being parallel to the z -axis with a typical length of 256 lattice sites and different diameters d . Due to shape as well as crystalline anisotropy the equilibrium magnetization is aligned with the long axis of the system. However, we start the simulation with an abrupt, head-to-head domain wall as initial configuration, letting the wall relax until a stable state

is reached. The distance of the initial wall position from the end is approximately 1/3 of the system length. Then we switch on the driving magnetic field B along the easy axis and wait until a stationary state is reached for some time interval in which the velocity v of the wall is constant while the wall is moving through the central part of the wire. We calculate the domain wall velocity from the magnetization versus time data, averaged over a period of time where no influence of the finite system size on the domain wall can be observed, i. e. until the wall approaches the other end of the wire.

Inspection of the stationary state of the moving domain wall shows that, depending on the ratio ω/J , either transverse domain walls or vortex walls are found. Representative spin configurations are shown in Fig. 1. The transverse domain wall (left hand side) is observed for diameters smaller than the exchange length $d_{ex}/a = \pi\sqrt{J/(6\omega\zeta(3))}$ of the system [10] where $\zeta(3) \approx 1.2$ is Riemann's Zeta-function (see also [11] for the exchange length in continuum theory where $3\zeta(3)$ is replaced by π). Here all spins within cross-sectional planes perpendicular to the wire axis are parallel so that the system is effectively one dimensional. Note, that the spin precession leads to a rotation of the spin direction within the wall while it is moving.

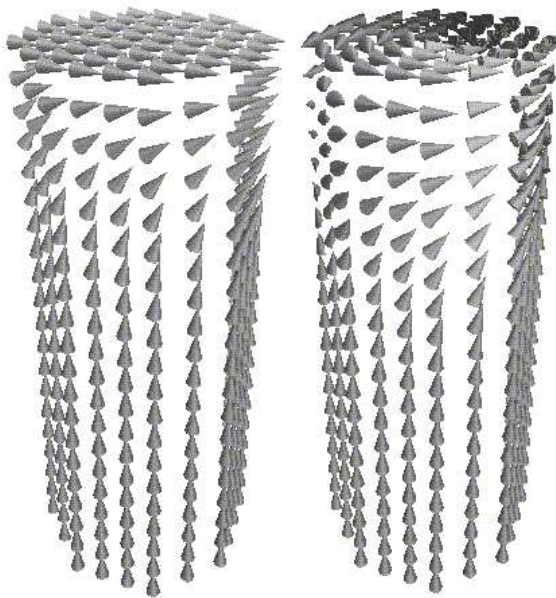


FIG. 1: Snapshots of a transverse (left, $\omega/J = 0.003$) and a vortex (right, $\omega/J = 0.2$) wall. The diameter $d = 8$ is kept constant while the exchange length of the system is varied. Shown is only a part of the system below the current wall position. $D_e/J = 0.05$.

With increasing dipolar interaction, a crossover to a vortex wall sets in (right hand side of Fig. 1) which is now energetically favorable since the vortex structure leads to a flux closure. These findings are in agreement with corresponding spin model simulations of thermally activated reversal [10] and micromagnetic results [12, 13]

obtained from simulations of the LLG equation using a micromagnetic continuum model.

In the following we turn to the investigation of the influence of the domain wall width and structure on its velocity. Fig. 2 compares the dependence of the domain wall width Δ and domain wall velocity v on the strength of the dipolar coupling. Here, the domain wall width was determined numerically by fitting a tanh-profile to the easy axis magnetization of the moving wall in the stationary state where the magnetization is averaged over cross-sectional planes. However, it should be mentioned that for large dipolar interaction in a vortex wall the wall profile cannot accurately be described by a simple tanh-profile. Note, that even in the limit $\omega \rightarrow 0$ the wall is stabilized by the additional crystalline anisotropy D_e .

For a spin chain ($d = 1$) the domain wall is necessarily always planar while for the system with larger diameter a crossover to a vortex wall occurs. The crossover can be identified as a jump of the domain wall velocity for the $d = 8$ data. Fig. 2 demonstrates that for a transverse wall the domain wall velocity is proportional to the wall width. For a vortex wall this is at least qualitatively the case. Width and velocity of transverse walls decrease with increasing dipolar interaction while for vortex walls the opposite is true. The crossover itself leads to a jump of the wall velocity not the wall width.

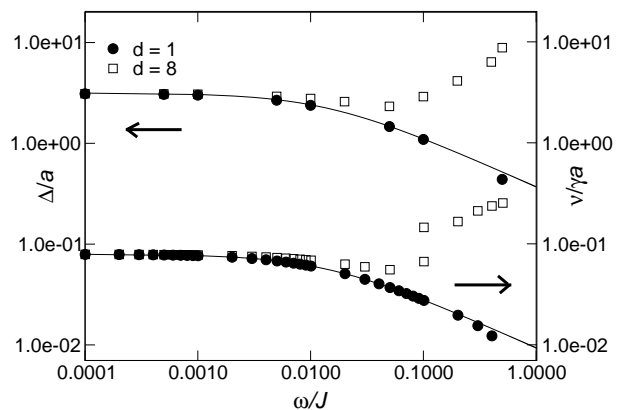


FIG. 2: Domain wall velocity and domain wall width versus dipolar coupling for a spin chain and a cylindrical system, respectively. $D_e/J = 0.05$, $\mu_s B/J = 0.05$, $\alpha = 1$. The solid lines correspond to Eqs. 4 and 3, error bars are smaller than the symbol size.

For a transverse wall the domain wall velocity is well described by an equation derived by Slonczewski as the lower limit for one-dimensional domain wall motion [5],

$$v = \frac{\gamma}{\alpha + 1/\alpha} \Delta_B B. \quad (3)$$

Here, Δ_B is the well-known Bloch wall width

$$\Delta_B = a \sqrt{\frac{J}{2(D_e + 3\omega\zeta(3))}}, \quad (4)$$

where, for our case, the denominator $D_e + 3\omega\zeta(3)$ estimates the effective anisotropy coming from shape as well as crystalline contributions (as before in a continuum theory $3\zeta(3)$ is replaced by π). Both equations above are drawn in Fig. 2 as solid lines and they agree very well with the numerical data for transverse walls.

In the following we focus on the mobility of vortex walls. The crossover from transverse to vortex wall can also be observed while varying the diameter of the system keeping the exchange length constant. Since for sufficiently small driving fields the domain wall velocity is proportional to the field in Fig. 3 we directly show the domain wall mobility dv/dB versus diameter of the system. Obviously there are two distinct regions with distinct wall mobility behavior. For low diameters where the transverse wall is found the system behaves effectively one-dimensional and in the limit $d \rightarrow 1$ the domain wall mobility follows Eq. 3. With increasing diameter the observed width of the transverse domain wall increases little due to the dipolar interaction leading to small deviations from the analytic Slonczewski result assuming a Bloch wall width. Nevertheless, we confirmed numerically, that Eq. 3 is still valid when the Bloch wall width Δ_B is replaced by the actual (numerically determined) width of the transverse wall.

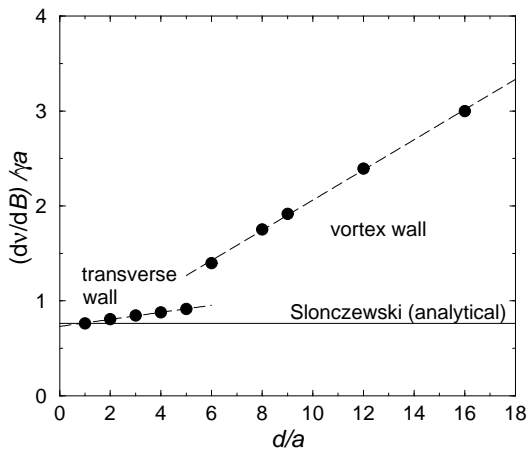


FIG. 3: Domain wall mobility versus diameter of cylindrical systems. The model parameters are $\omega/J = 0.003$, $D_e/J = 0.1$, $\alpha = 1$. The constant line corresponds to Eq. 3, the dashed lines are guides to the eye, error bars are smaller than the symbol size.

Increasing the diameter of the system a crossover from transverse to vortex wall is observed with a drastic increase of the domain wall mobility. As seen in Fig. 2, the reason for this effect is not a comparably drastic change of the wall width. Instead, as we will discuss in the following for a vortex wall the domain wall mobility follows a law with a different dependence on the damping con-

stant, namely the Landau-Lifshitz formula [4],

$$\frac{dv}{dB} = \frac{\gamma}{\alpha} \Delta, \quad (5)$$

where in our case Δ is the actual domain wall width of the vortex wall. The equation above is a limit of the more general Walker equation [6, 7, 8],

$$v = \frac{\gamma Ba}{\alpha} \sqrt{\frac{J}{2(D_e + D_h \sin^2 \phi)}}, \quad (6)$$

which was derived for sufficiently small driving fields for a system with an additional hard-axis anisotropy D_h . This anisotropy forces the equilibrium magnetization into an easy plane. Walkers formula is valid as long as the spin motion takes place in one plane which is defined by a constant angle ϕ to the easy plane of the system. ϕ is given as

$$\sin \phi \cos \phi = \frac{\mu_s B}{\alpha 2 D_h}, \quad (7)$$

where this equation also defines a condition for the validity of the walker formula. For a given α there exists a maximum field value (or vice versa for a given field a minimum α value) beyond which the spin motion is no longer restricted to one plane and instead an irregular precessional motion starts [6]. Note, that the Landau-Lifshitz formula is the $\phi = 0$ limit of the Walker equation, i. e. the limit of a strong hard axis anisotropy which forces the spin motion into the easy plane.

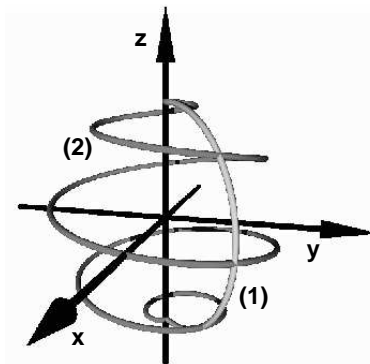


FIG. 4: Two different paths for the reversal of a spin. While (2) is dominated by precession, as in a transverse wall, the path (1) is restricted to one plane as in a vortex wall.

The equations above were derived for one dimensional systems and the question arises why these formula should be valid for the motion of a vortex wall with a non-uniform spin structure in cross-sectional planes. For a qualitative understanding we note that the motion of the spins within each spin chain which is parallel to the wire axis is indeed restricted to a certain plane passing through the spins positions. For a spin chain at the surface of the cylinder and in the limit of small driving fields

these are tangential planes of the cylinder surface. The responsible force which keeps the spin motion of each chain in this plane is for a vortex wall not a hard axis anisotropy — as in the original calculation — but the energetical principle which forms the vortex, i. e., the combination of exchange and dipolar interaction. Since this is the condition under which Walker's formula was derived it seems to be plausible that Eq. 6 describes the wall mobility in the case of an extended spin system as long as the spin motion during the reversal takes place in one plane. For a transverse wall, on the other hand, the situation is different: the precession of the wall leads to the fact that the motion of each single spin consists of precession and relaxation with no restriction to one single plane. These two different paths for the reversal of a spin are sketched in Fig. 4.

The main difference between Eqs. 3 and 5 is the dependence on damping. This is demonstrated in Fig. 5 which shows the ratio of the calculated wall mobility and the numerically determined domain wall width for two different strengths of dipolar interaction leading to the two different wall shapes. In the high damping limit both formulas agree. For a transverse wall the mobility shows a maximum at $\alpha = 1$ and for lower damping the domain wall mobility decreases with decreasing damping constant. In the limit $\alpha \rightarrow 0$ only a precession of the domain wall remains without an effective wall motion along the wire.

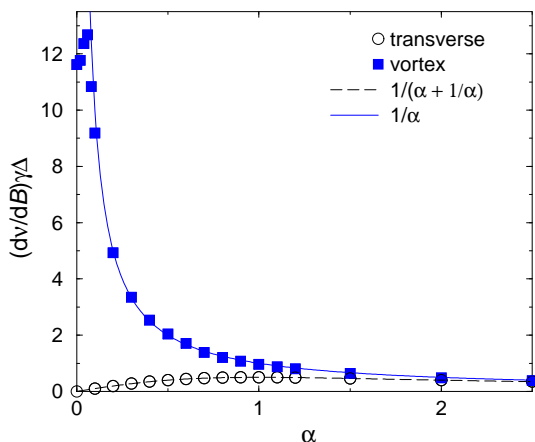


FIG. 5: Reduced domain wall mobility versus damping constant. The model parameters are $\omega/J = 0.01$ (transverse wall) and $\omega/J = 0.7$ (vortex wall) respectively, $D_e/J = 0.05$, $\mu_s B/J = 0.05$, $d = 4$. Error bars are smaller than the symbol size.

For a vortex wall the domain wall mobility increases with decreasing damping constant following a $1/\alpha$ law as long as one is above a critical value α_c . As was discussed in connection with Eq. 7 this value α_c sets the limit of pure relaxational spin motion. As was discussed before, the role of the hard axis anisotropy D_h in Eq. 7

in our case is played by the combination of exchange and dipolar interaction which forms the vortex and forces the spin motion into one plane. We would like to stress that for experimental systems the low damping limit is more relevant. Here, the difference between the two domain wall mobilities (reduced to the domain wall width) can be extremely large, up to a factor of $1/\alpha^2$.

For smaller values of α below the critical one the mobility decreases again and finally converges to a finite value since even for $\alpha = 0$ the wall can move. In this limit the LLG equation conserves the energy of the system, and lowering the Zeeman energy leads to an increase of exchange energy, leaving an excited spin system behind the wall. These observations are also in agreement with the calculations of Walker [6].

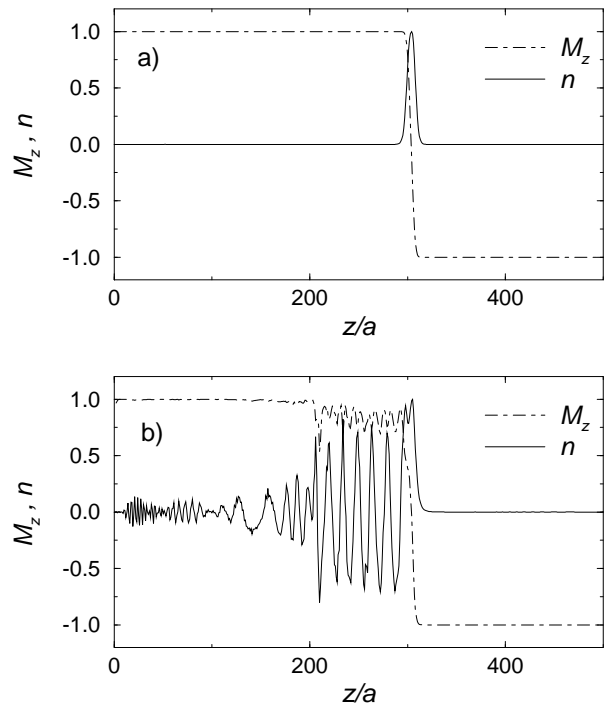


FIG. 6: Profiles and winding numbers of moving vortex walls in a) the high damping limit ($\alpha = 1$) and b) the low damping limit ($\alpha = 0$). $d = 8$, $\omega/J = 0.2$, $D_e/J = 0.05$, $\mu_s B/J = 0.1$

This effect is demonstrated in Fig. 6. Here, profiles of the moving walls are shown as well as the so-called winding number

$$n = \frac{1}{2\pi R} \int (\text{rot} \underline{S})_z dx dy$$

which is calculated numerically over all perpendicular planes of the wire. The winding number is a measure for the existence of vortices. $n = 1$ means that all spins along the boundary are aligned building a ring with perfect flux closure. Fig. 6 a) shows the high damping limit with a perfect vortex in the center of the wall. In the very low-damping limit, Fig. 6 b) the situation is much more

complicated. Here, behind the moving wall (smaller z) an excited spin system is left with vortex-type spin waves which are ejected from the moving wall.

To conclude, in agreement with prior work [10, 12, 13] we have found different wall structures for driven domain walls in cylindrical systems, transverse and vortex walls, depending on the diameter of the system as compared to the exchange length of the given material. While for vortex walls the domain wall velocity is described by the formula from Walker, transverse walls follow a formula from Slonczewski. In both cases the domain wall velocity is proportional to the domain wall width. The main difference is the dependence on the damping constant. For small values of the damping constant this difference can lead to drastic differences where the velocity of the vortex wall is up to a factor of $1/\alpha^2$ larger. The reason

for this difference is probably the fact that each spins motion in the case of the vortex wall is completely within one single plane as it is the case for the model where the Walker formula was derived for, while this is not the case for a transverse wall where the precession of the wall leads to a three dimensional spin motion.

Acknowledgments

The authors thank D. Garanin and S. Lübeck for helpful discussions. This work has been supported by the Deutsche Forschungsgemeinschaft (SFB 491 and NO290).

-
- [1] C. A. Ross, R. W. Chantrell, M. Hwang, M. Farhoud, T. A. Savas, Y. Hao, H. I. Smith, F. M. Ross, M. Redjail, and F. B. Humphrey, *Phys. Rev. B* **62**, 14252 (2000).
 - [2] K. Nielsch, R. B. Wehrspohn, J. Barthel, J. Kirschner, S. F. Fischer, H. Kronmüller, T. Schweinböck, D. Weiss, and U. Gösele, *J. Magn. Magn. Mat.* **249**, 234 (2002).
 - [3] T. Ono, H. Miyajima, K. Shigeto, K. Mibu, N. Hosoi, and T. Shinjo, *Science* **284**, 468 (1999).
 - [4] D. L. Landau and E. Lifshitz, *Phys. Z. Sowjetunion* **8**, 153 (1935).
 - [5] A. P. Malozemoff and J. C. Slonczewski, *Magnetic Domain Walls in Bubble Materials* (Academic Press, New York, 1979).
 - [6] N. L. Schryer and L. R. Walker, *J. Appl. Phys.* **45**, 5406 (1974).
 - [7] J. F. Dillon, in *Magnetism*, edited by G. T. Rado and H. Suhl (Academic Press, New York, 1963), Vol. 1, p. 149.
 - [8] D. A. Garanin, *Physica A* **178**, 467 (1991).
 - [9] U. Nowak, in *Annual Reviews of Computational Physics IX*, edited by D. Stauffer (World Scientific, Singapore, 2001), p. 105.
 - [10] D. Hinzke and U. Nowak, *J. Magn. Magn. Mat.* **221**, 365 (2000).
 - [11] A. Hubert and R. Schäfer, *Magnetic Domains* (Springer-Verlag, Berlin, 1998).
 - [12] H. Forster, T. Schrefl, D. Suess, W. Scholz, V. Tsiantos, R. Dittrich, and J. Fidler, *J. Appl. Phys.* **91**, 6914 (2002).
 - [13] R. Hertel, *J. Magn. Magn. Mat.* **249**, 251 (2002).